引用格式：LAI Junchi, HOU Shanglin, LEI Jingli, et al. Characteristics of Reflection Spectrum of Brillouin Dynamic Grating in Single Mode Fibers[J]. Acta Photonica Sinica, 2021, 50(7):0706005
赖俊池,侯尚林,雷景丽,等.单模光纤中布里渊动态光栅反射谱的特性[J].光子学报,2021,50(7):0706005

单模光纤中布里渊动态光栅反射谱的特性

赖俊池,侯尚林,雷景丽,李晓晓
(兰州理工大学 理学院,兰州 730050)

摘　要:基于受激布里渊散射和弹性声学理论,给出了布里渊动态光栅理论模型。基于光纤布拉格光栅理论,采用数值模拟的方法计算了布里渊动态光栅的反射谱,证明了布里渊频移引起的布拉格波长下移等于多普勒频移。计算了泵浦功率为0.1～30 W、脉宽为2～10 ns、单模光纤芯径为8～10 μm时的反射率和光谱宽度。当功率增长到30 W、脉宽达到10 ns时,峰值反射率分别达到2.17×10^{-6}和7.16×10^{-9};反射谱的光谱宽度随着脉冲宽度的增加而减小,当脉冲宽度为10 ns时,最小光谱宽度为1.2×10^{-4} nm;当纤芯直径减小到8 μm时,反射率增长到6.64×10^{-11}。计算结果表明,布里渊动态光栅的反射率与泵浦波的功率和脉宽呈正相关,与光纤的纤芯直径呈负相关;反射谱的光谱宽度不受泵浦波功率和纤芯直径的影响,但与脉冲宽度呈负相关。

关键词:受激布里渊散射;单模光纤;反射谱;光纤光栅;布里渊动态光栅
中图分类号:TN929.11　　**文献标识码**:A　　**doi**:10.3788/gzxb20215007.0706005

Characteristics of Reflection Spectrum of Brillouin Dynamic Grating in Single Mode Fibers

LAI Junchi, HOU Shanglin, LEI Jingli, LI Xiaoxiao
(*School of Science, Lanzhou University of Technology, Lanzhou* 730050, *China*)

Abstract: The Brillouin dynamic grating model is developed based on the stimulated Brillouin scattering and elastic acoustic theory. The reflection spectrum of the Brillouin dynamic grating is calculated based on the fiber Bragg grating theory, and it is demonstrated that the Bragg wavelength downshifts by Brillouin frequency shift equals the Doppler frequency shift. The reflectivity and the spectral width are calculated when the pump power ranges from 0.1 W to 30 W, the pulse width ranges from 2 ns to 10 ns and the core diameter of a single mode fiber ranges from 8 μm to 10 μm. When the power increases to 30 W and the pump pulse width reaches 10 ns, the peak reflectivity is 2.17×10^{-6} and 7.16×10^{-9}, respectively. The spectral width of the reflection spectrum decreases with the increase of pulse width. When the pulse width is 10 ns, the minimum spectral width is 1.2×10^{-4} nm. When the fiber core diameter decreases to 8 μm, the peak reflectivity increases to 6.64×10^{-11}. The results show that the reflectivity of the Brillouin dynamic grating is positive correlation with the power and the pulse width of the pump wave, but it is negative correlation with the core diameter of optical fiber. The spectral width of the reflection spectrum is not

---

Foundation item: The National Natural Science Foundation of China (No. 61665005), the Natural Science Foundation of Gansu Province of China (Nos. 17JR5RA132, 17JR5RA119), the HongLiu First-class Disciplines Development Program of Lanzhou University of Technology

First author: LAI Junchi (1995—), male, M.S. degree candidate, mainly focuses on optical fiber communication and sensing technology. Email: m18392991663@163.com

Supervisor(Contact author): HOU Shanglin (1970—), male, professor, Ph.D. degree, mainly focuses on optical fiber communication and sensing technology. Email: houshanglin@vip.163.com

Received: Dec.29, 2020; **Accepted**: Feb.24, 2021

affected by the power of the pump wave and the diameter of the fiber core, but it is negative correlation with the pulse width.

Key words: Stimulated Brillouin scattering; Single mode fiber; Reflection spectrum; Fiber grating; Brillouin dynamic grating

OCIS Codes: 060.2270; 290.5900; 230.1040; 190.4370

0 Introduction

Stimulated Brillouin Scattering (SBS) is a process that results from a form of coherent light-sound coupling[1-2]. SBS has attracted much attention and been investigated extensively since it was first observed experimentally in 1964[3]. The SBS occurring in optical fibers plays a very important role in optical telecommunication and optical sensing system. A strong pump wave is scattered when transmitting along optical fibers, and the Stokes waves are produced which frequency is downshifted. Because of the electrostriction in the optical fibers, the acoustic waves are formed running along the optical fiber. Since the acoustic wave is a kind of mechanical waves, the periodic variation of the refractive index along the optical fiber is formed when the acoustic wave propagates in the optical fiber. This spatial and temporal periodic modulation of the refractive index in optical fibers is known as a Brillouin Dynamic Grating (BDG) running along the fiber. BDG in optical fibers has been extensively studied due to its great potential that exploits acousto-optic interactions to create optical fiber sensing[4], variable optical delay[5], photonic chip[6], all-optical signal processing[7], high-precision optical spectrum analyzer[8] and so on.

Up to now, a lot of research work on the BDG in optical fibers has been reported both theoretically and experimentally. In 2008, SONG K Y[9-10] experimentally observed BDG in the polarization maintaining fiber, then his team successfully produced BDG in a single mode fiber, which has a narrower reflection bandwidth, large reflectivity, and is easier to control. In 2012, TAKIGAWA S and HORIGUCHI T[11] built a moving fiber gratings model to derived an approximate expression and realized an experimental observation in a coiled single mode fiber, and then experimentally generated BDG in a few mode fiber[12]. It was also reported that the BDG was produced by using chaotic laser in a polarization maintaining fiber[13]. Through reading the previous reference papers, it is concluded that the reported research work on the BDG in optical fibers mainly focused on the experimental study. This is because the refractive index modulation depends on the acoustic modes in optical fibers, the acoustic modes are very different from the optical modes in optical fibers which are determined by the waveguide structure and the material. So, the distribution of the acoustic modes is necessary for studying the BDG. Because the acoustic wave exists in the optical waveguide, there are many acoustic modes existing in the optical fiber. Thus, it is very difficult to model and theoretically study the BDG.

In this work, the acoustic modes in the single mode optical fiber are investigated and the BDG model is theoretically derived based on the SBS and elastic acoustic theory, the reflection spectrum of the BDG in single mode fibers is simulated, and the results are in agreement with the reported experimental results.

1 Theoretical model

1.1 Refractive index perturbation of BDG

The BDG in a single mode optical fiber can be treated as a moving refractive index grating along the optical fiber which is stimulated by a coherent acoustic wave field induced by SBS. Fig. 1 shows the conceptual illustration of the BDG operation in an optical fiber. Counter propagating waves, pump1 and pump2, have the same polarization and meet in the optical fiber, the frequency offset between two pump waves is set to the Brillouin frequency shift of the fiber. The acoustic wave is driven by the beating between the pump and stokes waves; the power of pump1 is greater than that of pump2; and a probe wave with the orthogonal polarization propagates in the direction of pump1 and is reflected by the BDG for detection[14].

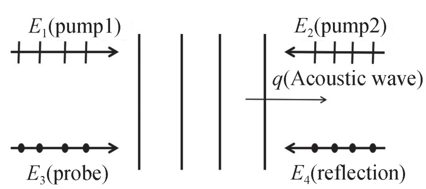

Fig. 1　BDG excitation and detection

The optical fields in Fig.1 can be represented as

$$\tilde{E}(z,t)=\sum_{i=1}^{4}\tilde{E}_i(z,t) \tag{1}$$

$$\tilde{E}_i(z,t)=A_i\mathrm{e}^{\mathrm{j}\left(k_i z-\omega_i t\right)}+\mathrm{c.c} \tag{2}$$

where $\tilde{E}(z,t)$ means the optical field varying with time and space, z represents the propagation direction of optical wave, t is the time when the optical wave moves along the propagation direction; $\tilde{E}_1(z,t)$, $\tilde{E}_2(z,t)$, $\tilde{E}_3(z,t)$, $\tilde{E}_4(z,t)$ represent the optical fields of pump1, pump2, probe and reflection waves, respectively; A_i is the amplitude of optical fields, k_i represents the wave vectors, ω_i represents the frequency of pump1, pump2, probe, reflection waves, respectively; c.c means complex conjugation. $\tilde{\rho}(z,t)$ is acoustic field, and can be expressed as[15]

$$\tilde{\rho}(z,t)=\Delta\rho\mathrm{e}^{\mathrm{j}(qz-\Omega t)}+\mathrm{c.c} \tag{3}$$

where $\Delta\rho$, q, Ω are the amplitude, wave vector, frequency of acoustic wave, respectively.

The frequency of acoustic wave equals Brillouin frequency shift Ω, which is given by

$$\Omega=\frac{2v}{c/n_{\mathrm{eff}}}\omega_1 \tag{4}$$

where v is the velocity of acoustic wave, c is the velocity of light in vacuum, ω_1 denotes the frequency of pump wave 1, and n_{eff} is the effective refractive index at the pump wavelength.

Applying Newton's second law to the volume element of fiber material, mechanics equation can be expressed by

$$\nabla P+\Gamma\rho_0 u+\rho\frac{\partial u}{\partial t}=\frac{1}{2}\varepsilon_0\gamma_{\mathrm{e}}\nabla(\tilde{E}^2) \tag{5}$$

where P is the pressure per unit volume, Γ means damping parameter, ρ_0 is the material density of medium, u is elastic velocity with propagation direction of the acoustic wave, ρ means the density after the propagation of acoustic wave. ε_0 is permittivity of vacuum and γ_{e} is electrostriction constant. The source term on the right-hand side of Eq. (5) consists of the divergence of the electrostrictive force. The continuity equation of elasticity can be given by[16]

$$\nabla\cdot u+\frac{1}{\rho_0}\frac{\partial\rho}{\partial t}=0 \tag{6}$$

We substitute Eq. (6) into the Eq. (5), one can obtain the result

$$\nabla^2 P-\Gamma\frac{\partial\rho}{\partial t}-\frac{\partial^2\rho}{\partial t^2}=\frac{1}{2}\varepsilon_0\gamma_{\mathrm{e}}\nabla^2(\tilde{E}^2) \tag{7}$$

The adiabatic modulus M is expressed as

$$M=\rho_0\frac{\partial P}{\partial\rho} \tag{8}$$

Then Eq. (7) can be formed as

$$\nabla^2\rho-\frac{\rho_0}{M}\Gamma\frac{\partial\rho}{\partial t}-\frac{\rho_0}{M}\frac{\partial^2\rho}{\partial t^2}=\frac{1}{2}\frac{\rho_0}{M}\varepsilon_0\gamma_e\nabla^2(\tilde{E}^2) \tag{9}$$

Based on the theory of elastic-acoustic, we can obtain

$$\frac{\rho_0}{M}=\frac{1}{v^2} \tag{10}$$

Then Eq. (7) can be written as

$$\nabla^2\rho-\frac{1}{v^2}\Gamma\frac{\partial\rho}{\partial t}-\frac{1}{v^2}\frac{\partial^2\rho}{\partial t^2}=\frac{1}{2v^2}\varepsilon_0\gamma_{\mathrm{e}}\nabla^2(\tilde{E}^2) \tag{11}$$

Suppose the two pump waves are all in x polarization, while the probe and the reflected waves are polarized in y direction, therefore there are only two terms left in the drive term of the acoustic field. The solution of equation under steady state condition is

$$\Delta\rho=\frac{1}{v^2}\varepsilon_0\gamma_{\mathrm{e}}A_1A_2 \tag{12}$$

The equation for the velocity of acoustic wave is conveniently expressed in terms of the compressibility C

$$v^2=\frac{1}{C\rho_0} \tag{13}$$

Brillouin scattering of optical wave by acoustic wave can be treated theoretically by considering the time-varying change $\Delta\tilde{\varepsilon}$ in the dielectric constant induced by the density variation $\Delta\tilde{\rho}$. It is usually assumed that $\Delta\tilde{\varepsilon}$ scales linearly with $\Delta\tilde{\rho}$, so that

$$\Delta\tilde{\varepsilon}=\frac{\partial\varepsilon}{\partial\rho}\tilde{\rho}=\gamma_e\frac{\tilde{\rho}}{\rho_0} \tag{14}$$

Substituting Eq. (3), Eq. (12) into Eq. (14), one can obtain the result

$$\Delta\tilde{\varepsilon}=(C\varepsilon_0\gamma_e{}^2A_1A_2)\mathrm{e}^{\mathrm{j}(qz-\Omega t)} \tag{15}$$

According to the third-order nonlinear effect, the refractive index can be defined as

$$\tilde{n}=\sqrt{\mathrm{Re}\left\{1+\chi^{(1)}+\chi^{(3)}\left|E(z,t)\right|^2\right\}} \tag{16}$$

The perturbation of refractive index associated with nonlinear effect can be expressed by

$$\Delta\tilde{n}=\frac{1}{2n_{\mathrm{eff}}}\mathrm{Re}(\chi^{(3)}) \tag{17}$$

The fluctuation in the susceptibility is then given by $\Delta\tilde{\chi}=\Delta\tilde{\varepsilon}$, Eq. (17) can be rewrite as

$$\Delta\tilde{n}=\frac{1}{2n_{\mathrm{eff}}}\Delta\tilde{\varepsilon}=\frac{\varepsilon_0\gamma_e{}^2C}{2n_{\mathrm{eff}}}A_1A_2\mathrm{e}^{\mathrm{j}(qz-\Omega t)} \tag{18}$$

Ignoring the imaginary part and only using real quantities, the refractive index variation of BDG can be obtained

$$\Delta\tilde{n}=\frac{\varepsilon_0\gamma_e{}^2CA_1A_2}{2n_{\mathrm{eff}}}\cos(\Omega t\pm qz) \tag{19}$$

Then the effective refractive index of fiber can be expressed as

$$n=n_{\mathrm{eff}}+\Delta\tilde{n} \tag{20}$$

It is simplified as

$$n=n_{\mathrm{eff}}+V\,\overline{\delta n_{\mathrm{eff}}}\cos\left(\Omega t\pm\frac{2\pi}{\Lambda}z\right) \tag{21}$$

where V is the fringe visibility of the refractive index change, $\overline{\delta n_{\mathrm{eff}}}$ means the index change spatially averaged over a grating period, Λ is grating period, which is actually wavelength of acoustic wave. It should be noted that the effective refractive index described by Eq. (21), is identical to the fiber Bragg grating.

1.2 Calculation method of reflectivity

According to the coupled-mode theory of the fiber Bragg grating, the amplitude reflection coefficient can be simply given by

$$r=\frac{-\kappa\sinh(\sqrt{\kappa^2-\hat{\sigma}^2}L)}{\hat{\sigma}\sinh(\sqrt{\kappa^2-\hat{\sigma}^2}L)+i\sqrt{\kappa^2-\hat{\sigma}^2}\cosh(\sqrt{\kappa^2-\hat{\sigma}^2}L)} \tag{22}$$

where κ, $\hat{\sigma}$ are AC, DC self-coupling coefficients, L means the effective length of the existing Brillouin grating[17]. They are expressed as respectively

$$L=\left(t_{\mathrm{P1}}+t_{\mathrm{P2}}\right)c/4n_{\mathrm{eff}} \tag{23}$$

$$\kappa=\frac{\pi}{2\lambda n_{\mathrm{eff}}}\varepsilon_0\gamma_e{}^2CA_1A_2 \tag{24}$$

$$\hat{\sigma}=2\pi n_{\mathrm{eff}}\Delta f/c \tag{25}$$

where t_{P1}, t_{P2} are the pulse widths of pump1 and pump2. Δf is the frequency shift of the probe wave from the center wavelength of reflection spectrum.

The reflectivity of fiber grating is expressed as

$$R=|r|^2=\frac{\sinh^2(\sqrt{\kappa^2-\hat{\sigma}^2}L)}{\cosh^2(\sqrt{\kappa^2-\hat{\sigma}^2}L)-\frac{\hat{\sigma}^2}{\kappa^2}} \tag{26}$$

The maximum reflectivity can be expressed as

$$R_{\max} = \tanh^2(\kappa L) \tag{27}$$

1.3 Doppler effect of the BDG

The BDG moves running along the optical fiber at the acoustic speed of v, then the reflective wave is influenced by the Doppler effect, thus the frequency of reflective wave downshifts which is given by

$$\omega' = \omega_{\mathrm{p}} \left[\left(\frac{c}{n_{\mathrm{eff}}} + v \right) \Big/ \left(\frac{c}{n_{\mathrm{eff}}} - v \right) \right]^{\frac{1}{2}} \tag{28}$$

where ω' is the frequency of reflection wave, ω_{p} is the frequency of pump wave, when the grating is away from the observer, v is negative, the frequency of stokes wave downshifts, on the contrary, v is positive, the anti-stokes wave whose frequency upshifts is produced.

2 Simulation results and discussions

SBS occurs in a single mode fiber whose parameters are shown in Table 1. In our simulation, two short pulses are utilized as the pump waves and are initially with powers of 0.1 W and width of 2 ns. Fig. 2 shows the distribution of acoustic mode. It can be seen that all kinds of acoustic modes are mainly confined in the core[18-19]. Thus, the optical and the acoustic waves are overlapped well in the core region of the single mode fiber to generate and enhance the BDG. Fig. 3 describes the reflection spectrum of the BDG in the single mode fiber. Because the BDG is a kind of weak fiber grating, the spectral width and the reflectivity are relatively small. The maximum reflectivity is 2.41×10^{-11}, with a spectral width of 3.5×10^{-4} nm. The Brillouin frequency shift is 11.123 1 GHz; the Doppler frequency shift is 11.122 8 GHz; the difference between them is 0.319 MHz. The Main reason for the error is due to the calculation accuracy. Fig. 4 shows the reflection spectrum using Brillouin frequency shift and Doppler frequency shift as the frequency shifts of reflected wave. It is clear that the frequency of reflected wave is shifted downward due to the Doppler effect, and the values of the Doppler frequency shift is equal to the Brillouin frequency shift.

Table 1 The parameters in a single mode fiber

Physical significance	Value
Density/($\mathrm{g \cdot cm^{-3}}$)	2.2
Acoustic velocity/($\mathrm{m \cdot s^{-1}}$)	5 970
Core diameter/μm	8~10
Cladding diameter/μm	125
Refractive index (1 550 nm)	1.443 96

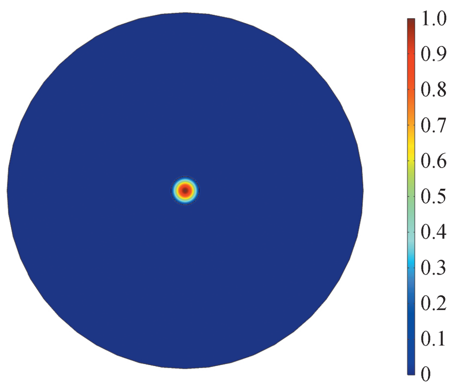

Fig. 2 Distribution of the acoustic mode

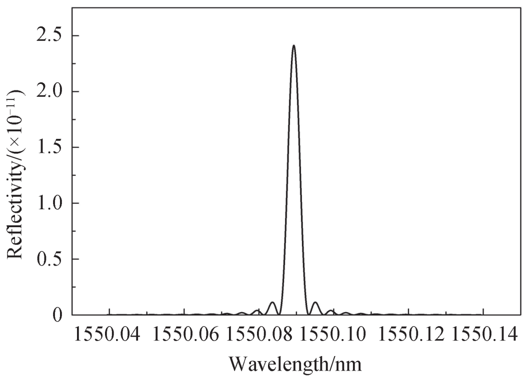

Fig. 3 Reflection spectrum of Brillouin dynamic grating

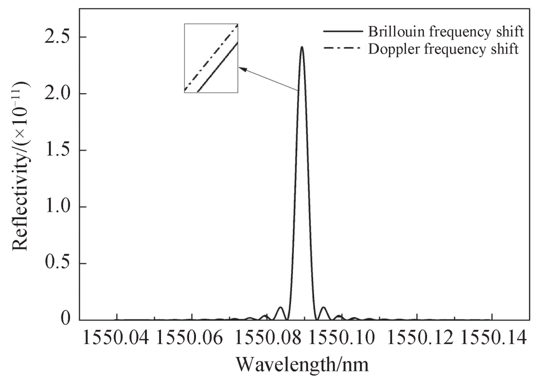

Fig. 4 Reflection spectrum by Brillouin frequency shift and Doppler shift

Fig. 5 depicts the temporal and spatial distribution of the refractive index perturbations. It clearly indicates that there are periodic variations of perturbation along with the temporal and spatial change. The spatial variation indicates that the distribution of the refractive index is similar to that of the Bragg grating, and the temporal variation shows that the BDG is a sort of moving fiber Bragg grating.

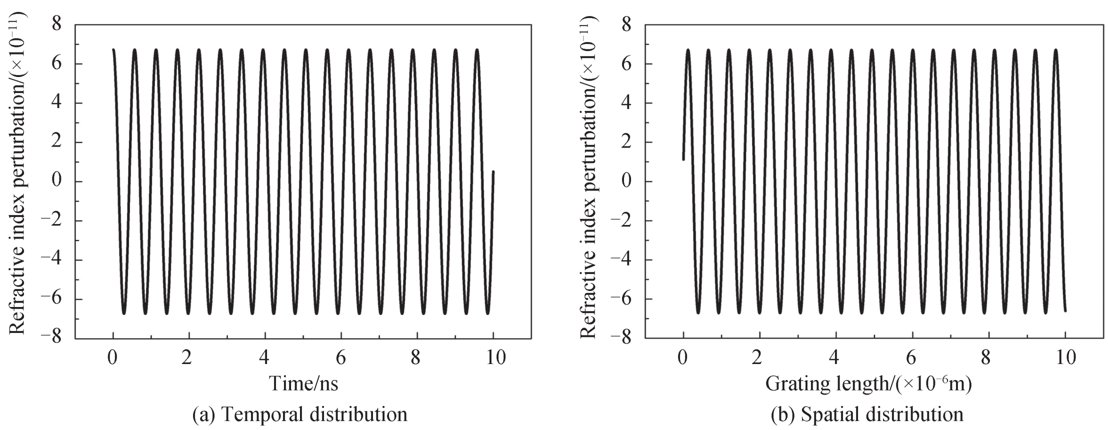

Fig. 5 Temporal and spatial distribution of refractive index perturbation

In the SBS, there is a Brillouin frequency shift between two pump waves, and the energy is transferred from the high frequency to the low frequency. According to the Eq. (19), the multiplication of electric field amplitude of two pump waves modulates the refractive index. So, the change of pump1 power plays the same part as the pump2 power. The variation of BDG′s reflectivity concerning the pump1 power is shown in Fig. 6 and Fig. 7. Fig. 6 depicts the reflectivity as a function of the pump power for a pulse width of 2 ns. It is obvious that the reflectivity of the BDG varies significantly with the pump power as more pump power is applied, but the change in the spectral width is negligible. The sidelobe of the reflection spectrum is caused by the non-uniform distribution of the refractive index in the optical fiber. The variation of refractive index at both ends of the BDG produces the sidelobe. The perturbation of the refractive index is relatively weak when the power of the pump wave is small. As the power increases, the perturbation becomes violent, which makes the sidelobe gradually increases. We can see from Fig. 7 that when the pump power increases to 30 W, the peak reflectivity also enhanced, but the relationship between the power and reflectivity is non-linear and grows rapidly. When the pump power reaches 30 W, the maximum reflectivity can be as high as 2.17×10^{-6}. It is because the stimulated Brillouin amplification becomes violent as the power of pump1 increases, the refractive index perturbations increase with the growth of pump power 1, the grating intensity is greatly extended, this enhances the reflection of BDG. These results are in agreement with the similar experiments[10-11,14].

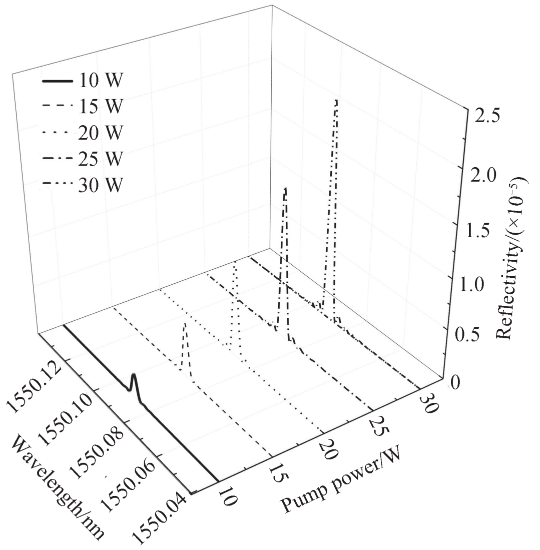

Fig. 6 Reflection spectrum of different pump power

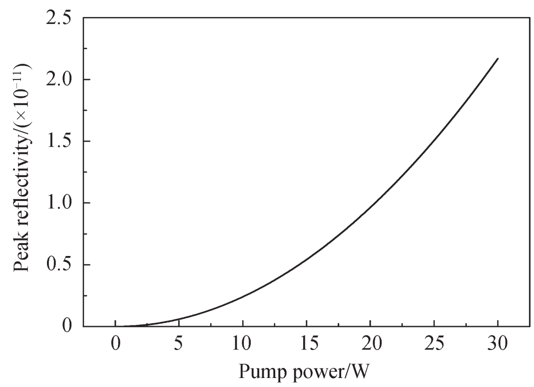

Fig. 7 Peak reflectivity as a function of pump power

The interaction time of the two pump waves extends as the pulse width increases, and the grating length also enhances. More energy of the incident wave is converted into the reflected wave as the grating length increases. In SBS, the increment in grating length induces actually a growth in the range of SBS effect. According to Eq. (23), the pulse width of pump1 and pump2 affects the length of BDG. As shown in Fig. 8, the pulse width also affects the reflectivity and the bandwidth of the reflection spectrum. The grating length increases with the growth of the pulse width, and the increment of the grating length leads to an enhancement of reflectivity, but the spectral width decreases accordingly. The refractive index varies with the position of BDG. The growth of the grating length induced the non-uniform distribution of the refractive index. The sidelobe becomes more significant. Fig. 9(a) shows that the spectral width as a function of the pump pulse width, the spectral width decreases from 3.5×10^{-4} nm to 1.2×10^{-4} nm with growth of pulse width. Fig. 9(b) depicts that the peak reflectivity as a function of the pump pulse width, when the pulse width is 10 ns, the maximum reflectivity is 7.16×10^{-9}. The results agree well with the theory of the weak fiber grating[20]. It also can be presumed that BDG is reinforced when continuous wave is utilized as pump wave, because the Brillouin grating can exist in the whole fiber.

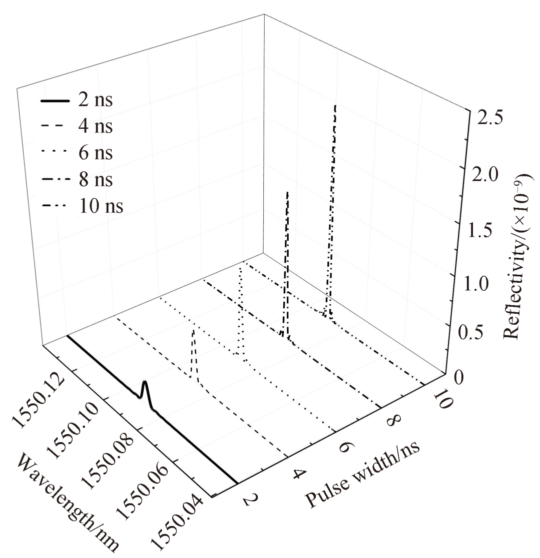

Fig. 8 Reflection spectrum of different pulse width

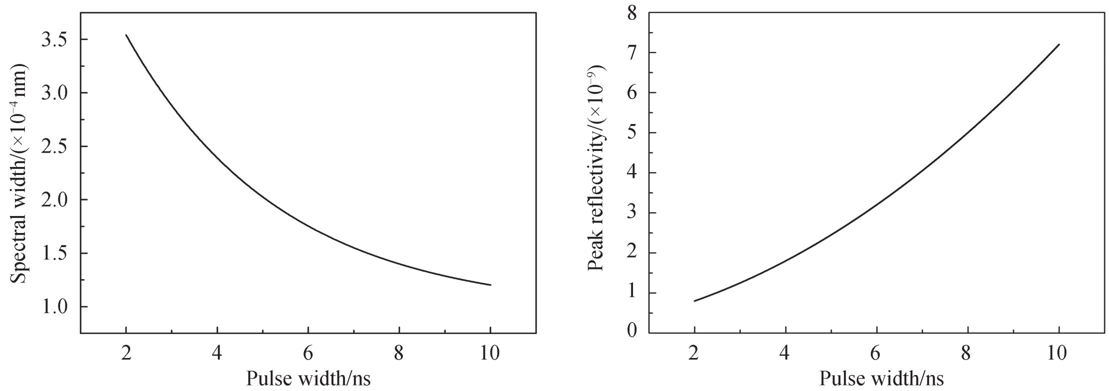

(a) Spectral width varying with the pulse width (b) Peak reflectivity varying with the pulse width

Fig. 9 The spectral width and the peak reflectivity as a function of pump pulse width

Fig. 10 and Fig. 11 describe the reflectivity as a function of core diameter. It can be seen that the reflectivity decreases with the growth of core diameter, but the alteration of the spectral width can be ignored. BDG is also enhanced with the reduction of core diameter due to the tight confinement of both optical and acoustic fields in the fiber core. This also suggests that Brillouin interactions could be greatly magnified in the small core of the optical fiber.

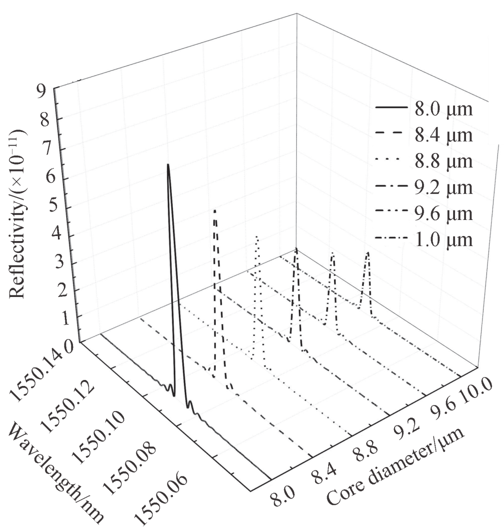

Fig. 10 Reflection spectrum of core diameter

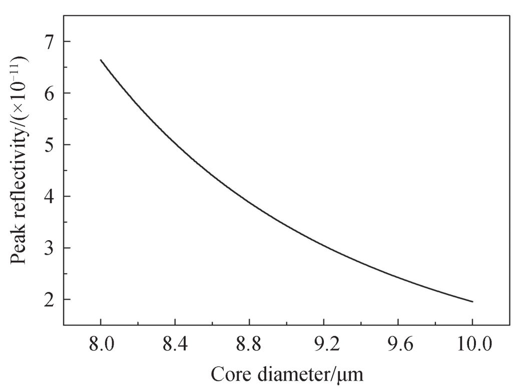

Fig. 11 Peak reflectivity as a function of core diameter

It is known from the above analysis that the reflectivity of the BDG is enhanced by tailoring the pump power, the pulse width and the core diameter. The maximum reflectivity can reach up to 6.63×10^{-5} with the pump power of 30 W, the pulse width of 10 ns and the core diameter of 8 μm. The reflectivity is still so small that it limits the application of BDG. For example, BDG is hard to introduce into the optical fiber amplifier because the amplifier needs fiber grating with high reflectivity to improve the pump conversion efficiency. But the BDG can be used as the optical fiber sensors in sensing. The BDG with low reflectivity can increase the capacity of the sensor, the wave at the same wavelength is not fully reflected and can be reused in a fiber.

3 Conclusion

In summary, the model of BDG is established, and the expression of refractive index perturbation is derived in this paper, the reflection spectrum of BDG in single mode fibers is investigated, the inference that Brillouin frequency shift is from the Doppler frequency shift is verified by the simulation result. The reflectivity is positive correlation with the pump power and pulse width, but it is negative correlation to the core diameter. The spectral width is not affected by the power of pump waves, but it is negative correlation to the pulse width and core diameter. The analysis results are in keeping with some experimental reports. BDG offers great promise for a range of applications, because it can be conveniently produced at any positions with variable length, which can be harnessed as optical communication, optical storage, and so on.

References

[1] LI Lijun, HOU Shanglin, LEI Jingli, et al. Slow light of stimulated brillouin scattering in few-mode fibers[J]. Acta Photonica Sinica, 2019, 48(5): 0506001.

[2] MA Yuanyuan, HOU Shanglin, LEI Jingli, et al. SBS fast light with low pulse distortion at doublet pumps in optical fibers [J]. Acta Photonica Sinica, 2019, 48(3): 0306002.

[3] CHEN Liang, ZHANG Wei, GAO Panyun, et al. Characteristics of forward stimulated Brillouin scattering effect in silica fibers with different microstructures[J]. Optik, 2019,179:82-88.

[4] XU Zhiniu, ZHAO Lijuan, CHEN Feifei, et al. Temperature and strain sensing mechanism in polarization maintaining fiber based on Brillouin dynamic grating[J]. Acta Photonica Sinica, 2019, 48(8): 0806001.

[5] SONG K Y, LEE K, LEE S B. Tunable optical delays based on Brillouin dynamic grating in optical fibers[J]. Optics Express, 2009, 17(12):10344-10349.

[6] PANT R, LI E, POULTON C G, et al. Observation of Brillouin dynamic grating in a photonic chip[J]. Optics Letters, 2013, 38(3):305-307.

[7] SANTAGIUSTINA M, CHIN S, PRIMEROV N, et al. All-optical signal processing using dynamic Brillouin gratings [J]. Scientific Reports, 2013, 3:1594.

[8] ZOU Weiwen, HE Zuyan, HOTATE K. Demonstration of Brillouin distributed discrimination of strain and temperature using a polarization-maintaining optical fiber[J]. Photonics Technology Letters, 2010, 22(8):526-528.

[9] SONG K Y, HOTATE K. All-optical dynamic grating generation based on Brillouin scattering in polarization maintaining fiber[J]. Optics Letters, 2008, 33(9):926-928.

[10] SONG K Y. Operation of Brillouin dynamic grating in single-mode optical fibers[J]. Optics Letters, 2011, 36(23):4686-4688.

[11] TAKIGAWA S, HORIGUCHI T. Reflection properties of Brillouin dynamic gratings in coiled single-mode fibers[C]. OFS2012 22nd International Conference on Optical Fiber Sensor, International Society for Optics and Photonics, 2012.

[12] LI Shenping, LI Mingjun, VODHANEL R S. All-optical Brillouin dynamic grating generation in few-mode optical fiber [J]. Optics Letters, 2012, 37(22):4660-4662.

[13] ZHANG Jianzhong, LI Zhuping, ZHANG Mingjiang, et al. Characterization of Brillouin dynamic grating based on chaotic laser[J]. Optics Communications, 2017, 396:210-215.

[14] DONG Yongkang, CHEN Liang, BAO Xiaoyi. Characterization of the Brillouin grating spectra in a polarization-maintaining fiber[J]. Optics Express, 2010, 18(18):18960-18967.

[15] AGRAWAL G P. Nonlinear fiber optics (fifth edition) [M] New York: Elsevier, 2013.

[16] BALDWIN G C. An introduction to nonlinear optics[M]. New York: Plenum Press,1969.

[17] DONG Yongkang, CHEN Liang, BAO Xiaoyi. Truly distributed birefringence measurement of polarization-maintaining fibers based on transient Brillouin grating[J]. Optics Letters, 2010, 35(2):193-195.

[18] WU Dongming, HOU Shanglin, LEI Jingli, et al. Superluminal propagation induced by forward stimulated Brillouin scattering in small-core photonic crystal fibers[J]. Acta Photonica Sinica, 2020, 49(7): 0706002.

[19] LI Qiangqiang, HOU Shanglin, LIU Yanjun, et al. Influence of acoustic wave on Stokes wave of guide acoustic wave Brillouin scattering in fibers[J]. Acta Photonica Sinica, 2016, 45(1): 0106004.

[20] ERDOGAN T. Fiber grating spectra[J]. Journal of Lightwave Technology, 1997, 15(8):1277-1294.